Waste Management 205 (2025) 115005

Contents lists available at ScienceDirect

Waste Management

journal homepage: www.elsevier.com/locate/wasman

Research Paper

Upcycling onion peels for enhanced gas barrier and antioxidant bioplastics based on starch from potato processing slurries

Mariana Vallejo [a], Beatriz Esteves [b], Pedro Carvalho [b], Manuel A. Coimbra [c], Martinho Oliveira [a,d], Paula Ferreira [a], Idalina Gonçalves [a,*]

[a] CICECO – Aveiro Institute of Materials, Department of Materials and Ceramic Engineering, University of Aveiro, 3810-193, Aveiro, Portugal
[b] CICECO – Aveiro Institute of Materials, Department of Chemistry, University of Aveiro, 3810-193, Aveiro, Portugal
[c] LAQV-REQUIMTE, Department of Chemistry, University of Aveiro, 3810-193 Aveiro, Portugal
[d] ESAN – School of Design, Management and Production Technologies, University of Aveiro, Santiago de Riba-Ul, Oliveira de Azeméis, Portugal

A B S T R A C T

The upcycling of food waste into high-value materials presents a key opportunity for sustainable waste management. While onion peel (OP) extracts have been investigated as additives for bioplastics, this study explores the direct incorporation of whole powdered OP (5–20 wt%) into starch-based films, eliminating extraction steps and fully valorizing this agro-industrial by-product. Using starch recovered from potato processing slurries as the polymeric matrix, the influence of OP on film structure, mechanical performance, water resistance, gas permeability, and antioxidant activity was evaluated. Chemical analysis of OP revealed a composition of 47% alcohol insoluble compounds (mainly pectin and cellulose), 12% alcohol soluble matter (primarily glucose-based carbohydrates), 6% lipids, 2% proteins, 5% gallic acid equivalents, and 27% ashes. The direct incorporation of powdered OP resulted in natural pigmentation, producing transparent films with an orangish hue. This approach enhances the aesthetic properties of films while eliminating the need for artificial dyes, contributing to a more sustainable product design. The developed bioplastics exhibited enhanced mechanical properties and improved water resistance, making them attractive for sustainable packaging applications. At OP concentrations above 10 wt%, Young's modulus increased from 1214 MPa to 1496 MPa, while tensile strength and elongation at break decreased from 31.4 MPa to 24.6 MPa and from 4.5% to 2.1%, respectively. Water contact angles increased from 75° up to 87°, and water vapor permeability was reduced by up to 60%, improving moisture resistance. Importantly, OP incorporation did not compromise oxygen (O_2), carbon dioxide (CO_2), or nitrogen (N_2) barrier properties and imparted significant antioxidant activity, with 20 wt% OP-based films inhibiting 93% of the 2.2′-azinobis-(3-ethylbenzothiazoline-6-sulfonic) acid radical cation ($ABTS^{\cdot+}$) after 6 h. This study presents an innovative waste-to-resource strategy that eliminates processing waste, aligns with circular economy principles, and demonstrates the first use of whole OP as a multifunctional additive in starch-based bioplastics. By replacing conventional extraction-based approaches, this method enhances material sustainability while promoting a scalable, zero-waste approach to packaging development.

1. Introduction

The food industry generates a substantial amount of organic waste, including by-products from crop processing, such as onion peels, which are often discarded and pose environmental challenges (Berenguer et al., 2023). However, these byproducts are rich in polysaccharides, lipids, proteins, phenolic compounds, and inorganic matter, among others, offering potential for various applications, including in sustainable packaging materials (Bhargava et al., 2020; Lopes et al., 2021; Oliveira et al., 2021).

Among the plethora of agricultural commodities, onions emerge as a cornerstone crop, commanding a global production exceeding 98 million tons annually (Stoica et al., 2022). Yet, a staggering 550,000 tons of onion peel, usually containing toxic sulfur compounds, mainly alk(en)yl cysteine sulfoxides, which naturally derive from the multilayer tissue of onion bulbs (Shabir et al., 2022). High sulfur content renders these peels unsuitable for human and animal consumption, precipitating biological and environmental conundrums exacerbated by the proliferation of phytopathogens like *Sclerotium cepivorum* (Chadorshabi et al., 2022; Kumar et al., 2022; Michalak-Majewska et al., 2020; Thivya et al., 2022). To face this challenge, the utilization of onion peel (OP) as a resource of bioactive compounds has been considered for anti-asthmatic, anticarcinogenic, and hypocholesterolemic therapeutic properties effects, (Abhiram Siva Prasad Pamula et al., 2021; Sagar et al., 2021), food preservatives (Michalak-Majewska et al., 2020; Sagar et al., 2021), and active textiles (Pucciarini et al., 2019) and biobased plastics (Lopes et al., 2021). In this last field, OP-derived extracts have been used as active additives for Krasch gum– (Liang et al., 2018), gelatin- (Uçak et al., 2019), carboxymethylcellulose- (Pagano et al., 2020), methylcellulose- (Gulati et al., 2023), chitosan- (Wang et al.,

* Corresponding author at: Department of Materials and Ceramics Engineering, University of Aveiro, 3810-193 Aveiro, Portugal.
E-mail address: idalina@ua.pt (I. Gonçalves).

https://doi.org/10.1016/j.wasman.2025.115005
Received 23 November 2024; Received in revised form 2 July 2025; Accepted 4 July 2025
Available online 12 July 2025

2022b), alginate- (Santos et al., 2021), gluten/alginate/cellulose- (Thivya et al., 2022), starch/k-carrageenan- (Wang et al., 2022a), and starch-based matrices (Boccalon et al., 2022). Overall, these studies showed that OP-derived extracts conferred natural pigmentation, antioxidant and antimicrobial activity, and pH sensitivity to the polysaccharide-based materials, while increasing their tensile strength. Despite these advancements, from the extraction of bioactive extracts remains an unvalued residue, which underscores the imperative research on novel avenues for the holistic utilization of OP.

This study proposes the direct incorporation of whole powdered OP into starch-based films as a novel waste valorization strategy. Unlike traditional extract-based approaches, this method utilizes the entire biomass, eliminating extraction steps and maximizing material utilization, while enhancing the films' gas barrier and antioxidant properties and contributing to sustainable waste management practices. Embracing the ethos of circular economy, starch derived from potato washing slurries was used as polymeric matrix. To assess this hypothesis, the influence of powdered OP content on chromatic, morphological, mechanical, water vapor and gas barrier, and antioxidant properties of starch-based films prepared via solvent casting was studied.

2. Materials and Methods

Brown onion peel (OP) and potato washing slurries were supplied by CALCOB and A Saloinha, Lda., two Portuguese companies dedicated to onion and potato chips production, respectively. Glycerol was purchased from Scharlab S. L. (Barcelona, Spain). Chloroform, *n*-hexane, and ethanol were obtained from Carlo Erba Reagents S.A.S. (Milan, Italy). Starch assay kit SA20, sodium azide, calcium chloride, ABTS reagent, and potassium persulfate were acquired from Sigma-Aldrich (Darmstadt, Germany). All purchased reagents were of analytical grade and used without further purification.

2.1. Milling of OP and recovery of starch from potato washing slurries

The onion peel (OP) was directly processed into powder through wet grinding, avoiding extraction steps and enabling full utilization of this agro-industrial by-product. This simplified method minimizes resource consumption, eliminates the need for solvents, and aligns with green chemistry principles while preserving OP's full range of bioactive compounds. The final suspension was then spray-dried at 120 °C using a pilot scale 9103 NIRO spray-drier (Dusseldorf, Denmark). The powdered and dried OP was then sieved using a stainless-steel sieve with a 75 μm mesh (Retsch, Haan W.Germany) and stored under dry conditions until use.

Starch was recovered from potato washing slurries by wet-sieving using a stainless-steel sieving set with meshes ranging from 150 μm to 300 μm (Retsch, Haan W. Germany) to remove small potato slices and peels. The recovered starch-rich aqueous suspension was then spray-dried at 120 °C using the NIRO 9103 spray-drier. The collected starch was sieved using a 150 μm mesh (Retsch, Haan W. Germany) and stored under dry conditions until further use (Oliveira et al., 2020).

2.2. Characterization of powdered OP and starch recovered from the potato washing slurries

2.2.1. Chromatic properties, particles size distribution, and morphology

Chromatic parameters were determined, in triplicate, using a portable Konica Minolta CR-400 colorimeter (New Jersey, USA). CIELab color profile was used to express the L^* (luminosity), a^* (red/green color), and b^* (yellow/blue color) chromatic coordinates. The total difference in color (ΔE) was calculated according to equation (1),

$$\Delta E = \sqrt{(\Delta L^*)^2 + (\Delta a^*)^2 + (\Delta b^*)^2} \quad (1)$$

where: ΔL^*, Δa^*, and Δb^* are the L^*, a^*, and b^* differences between films containing oil or waxes and the control films equation (Gonçalves et al., 2020).

The particles size distribution was determined through dynamic light scattering (DLS), using a Horiba LA-960 laser scattering particle size distribution analyzer (Kyoto, Japan). Before measurements, each suspended sample was ultrasonicated for 10 min to ensure the disruption of any particle agglomeration.

The particles shape was observed by scanning electron microscopy (SEM) using a Hitachi S4100 high-resolution field emission SEM (Tokyo, Japan). The samples were carbon coated under an argon atmosphere at 10 kV and 10 mA for 3 min using a Emitech K950X Polaron sputter coater (Chorley, United Kingdom) (Oliveira et al., 2020).

2.2.2. Chemical composition

Moisture content was determined using a KERN DBS60-3 humidity scale (Balingen, Germany).

Ashes content was determined in triplicate according to the AOAC Official Method 942.05 for ashes determination (AOAC Official method 942.05, 1998).

For determination of polysaccharides, an alcohol insoluble residue (AIR) was prepared through an aqueous extraction with 80% (V/V) ethanol for 20 min at 80 °C. Carbohydrate content was determined by GC-FID as alditol acetates, after a pretreatment with 12 M H_2SO_4, 3 h, 25 °C, followed by hydrolysis (1 M H_2SO_4, 2.5 h, 100 °C f or 2.5 h), reduction with $NaBH_4$ (15% w/V in 3 M NH_3, 1 h, 30 °C), and acetylation (acetic anhydride in the presence of 1-methylimidazole, 30 min, 30 °C). To estimate the uronic acids content, the 3-phenylphenol colorimetric method was used after the OP acid hydrolysis (Fernandes et al., 2019).

The protein content was determined by elemental analysis using a LECO's CHNS-932 Elemental Analyzer (Madrid, Spain) and the nitrogen content was converted into the protein percentage using a conversion factor of 6.25, following an adapted version of a described protocol (Fernandes et al., 2019; Gonçalves et al., 2021).

The lipid content of OP was determined based on the amount of waxes and oil. Waxes were extracted by a solid–liquid extraction using chloroform as solvent (Gonçalves et al., 2020). Briefly, OP was suspended in chloroform with a solid/liquid ratio of 10 g of OP per 50 mL and stirred for 24 h at 37 °C. Then, the solvent was removed under low pressure (70 hPa) and temperature (30 °C) using a Buchi rotatory evaporator R-114 (Flawil, Switzerland), until a constant weight was reached. The wax content was expressed as g of waxes per 100 g of OP. In turn, oil was independently extracted through Soxhlet using *n*-hexane as solvent and a solid/liquid ratio of 9 g OP per 150 mL of *n*-hexane. After 5 cycles at 80 °C, the solvent was removed under low pressure (70 hPa) and temperature (40 °C) using with the Buchi rotatory evaporator until constant weight [3]. The oil content was expressed in g of oil per 100 g of OP.

For the determination of total phenolics content, ASM of the OP was analyzed following a modified *Folin-Ciocalteu* method (Lopes et al., 2021), with the total phenolics content expressed in percentage of gallic acid equivalents (GAE).

The starch content was confirmed by amyloglucosidase hydrolysis, using the starch assay kit from Sigma.

All the measurements were carried out in triplicate.

2.2.3. Gelatinization profile and amylose/amylopectin content of starch

The gelatinization profile of starch was determined through differential scanning calorimetry (DSC) using a Chip DSC10 calorimeter from LINSEIS (Selb, Germany) (Gonçalves et al., 2020). Starch dispersions (30% w/V) were prepared in distilled water, transferred into stainless steel sealed crucible, and heated from 25 °C to 100 °C with a heating rate of 10 °C/min. The onset (T_o), peak (T_p), and conclusion (T_c) temperatures, and gelatinization enthalpy (ΔH) were directly obtained from DSC thermograms. All the measurements were carried out in triplicate.

For the determination of amylose content in the starch, the kit

"amylose/amylopectin assay procedure", K-AMYL 06/18 from Megazyme, (Bray, Irland) was used.

2.3. Preparation of starch- and starch/OP-based films

Starch (Control) and starch/OP-based films were prepared through casting, following a previously described method (Oliveira et al., 2020). Starch was pre-suspended in 200 mL of distilled water (4% w/V) and mixed with glycerol (30% w/w of dry starch weight) and OP at different contents (5% w/w, OP5, 10%, OP10, 15%, OP15, and 20%, OP20) at room temperature (24 °C ± 2 °C). The starch was gelatinized at 95 °C under continuous stirring at 200 rpm for 30 min. The resulting gelatinized suspension was then degassed using a Buchi V-600 vacuum pump (Flawil, Switzerland) at 100 hPa to remove entrapped air bubbles before casting. After degassing, 21 g of the gelatinized suspension was poured into plexiglass plates (144 cm^2, 3 mm depth). The films were dried under atmospheric conditions by solvent evaporation overnight in an air-ventilated oven at 25 °C ± 1 °C.". The films were then removed from the plates and stabilized at 24 °C ± 1 °C under controlled humidity atmosphere (54% RH) for at least 5 days until further characterization.

2.4. Characterization of starch- and starch/OP-based films

2.4.1. Chromatic properties and microstructure

The chromatic parameters of each film were determined, in triplicate, using a portable Chroma Meter (CR-400, Minolta, Japan), and calculated as described in section 2.3.1.

The surface and cross-section microstructures of the films were observed by SEM using Hitachi S4100 microscope (Tokyo, Japan). The samples were precoated coated under an argon atmosphere with a thin layer of carbon at 10 kV and 10 mA for 3 min.

2.4.2. Thickness and mechanical properties

The film was first cut into 5 cm x 1 cm strips, and their thickness was measured using a digital micrometer (Mitutoyo, Japan), at 5 different points throughout its length. For the mechanical performance evaluation, a Stable Micro Systems TA-XT plus C texture analyzer (Godalming, United Kingdom) was used. The tensile strength (TS), Youngs modulus (YM), and elongation at break (EAB) were determined by adapting the ASTM D 882–83 standard method, using a grip separation of 30 mm. The crosshead speed was maintained at a constant rate of 0.5 mm/s. TS, YM, and EAB were calculated following previously reported equations (Gonçalves et al., 2020). A minimum of 5 measurements were performed for each sample.

2.4.3. Water wettability

The surface water wettability of each developed film was determined through water contact angle (WCA) measurements using a Biolin Scientific Theta Lite optical tensiometer (Espoo, Finland). Five strips (5 x 1 cm) were cut in different parts of the film and a 3 μL of ultrapure water was dispersed onto each strip surface. The drops shape was analyzed for 10 s using the sessile drop fitting method and the contact angle was determined through the Young-Laplace method (Petronilho et al., 2021). At least 6 measurements on different parts of each strip were performed.

2.4.4. Gas barrier properties

2.4.4.1. Water vapor transmission rate. The film's water vapor transmission rate (WVTR) was determined through a gravimetric method, following an adaptation of the TAPPI Standard T-448 om-09. For that, each film was cut in 4 x 4 cm squares and sealed in a polypropylene cylindric cell with 2 cm diameter hole containing a dry desiccant (anhydrous calcium chloride pre-dried for 23 h at 200 °C) (Petronilho et al., 2021). Afterwards, the cell was stored at 24 °C ± 1 °C for 24 h in a desiccator with controlled relative humidity (54% ± 1%). Then, each cell was weighed and the WVTR was calculated using equation (2):

$$WVTR = \frac{\Delta m}{A \bullet t} \tag{2}$$

where Δm is the desiccant weight gain *(g)*, t is time for the weight gain (h), and A is available area for mass transfer (cm^2). The WVTR of each formulation was obtained by an average of 3 measurements.

2.4.4.2. Oxygen, nitrogen, and carbon dioxide permeability. The film's permeability to oxygen, nitrogen, and carbon dioxide was measured separately through the time-lag method at 30 °C (Bao et al., 2006; Fraga et al., 2018). The constant volume time-lag setup requires a step change in pressure upstream from the film (retentate) and monitoring of the pressure response downstream from the film (permeate). Membranes with 4,7 cm diameter were placed in the filter holder on top of a porous spacer that imposes no restriction to mass transfer. An *o*–ring was used, on top of the membrane to isolate the permeate from the retentate. The temperature was controlled, at 30 °C, by a heat-controlled ventilated oven with an uncertainty of (0.1 °C). The retentate and permeate pressures were measured by pressure transducers (Swagelok, Model S), with BFST of 0.25%. Prior to the measurements, the permeate followed by the retentate vapor phases were evacuated using a Buchi V-100 diaphragm vacuum pump (Essen, Germany). Then, the selected gas was introduced into the top storage compartment, still isolated from the membrane, at 1.7 bar, and the temperature was allowed to stabilize. Once stabilized (no pressure changes within 10 min), the gas was allowed to get in contact with the membrane, starting the measurement, and both the permeate and the retentate pressures were recorded with time, for 24 h. The relation between the permeate pressure (p_p) and the permeation time (t) is determined by equation (3) that describes the permeation of the gas through the film (linear region):

$$p_P = \frac{\mathrm{P{\cdot}A{\cdot}}R{\cdot}T{\cdot}p_f}{l{\cdot}V_P \bullet V_m}{\cdot}t - \frac{\mathrm{P{\cdot}A{\cdot}}R{\cdot}T{\cdot}p_f}{l{\cdot}V_P \bullet V_m}{\cdot}\frac{l^2}{6{\cdot}\mathrm{D}} \tag{3}$$

where P is the permeability given in Barrer (10^{-10} $cm^3_{STP}.cm.cm^{-2}.s^{-1}.cmHg^{-1}$), p_p (bar), p_f is the retentate pressure (bar), A is the area of the film available for mass transfer (cm^2), T is the temperature (°C) and R is the ideal gas constant l is the film thickness (cm), Vp is the permeate volume (cm^3), Vm is the gas molar volume (cm^3), and D is the diffusion coefficient. The permeability of the gas through the membrane can be determined by rearranging equation (3) slope, giving rise to equation (4):

$$P = \frac{l{\cdot}V_p \bullet V_m{\cdot}m}{A{\cdot}R{\cdot}T{\cdot}p_f} \tag{4}$$

where m is the slope of equation (3).

2.4.5. Water solubility and swelling

The water solubility of each film was analyzed, in triplicate, in an aqueous medium through weight loss measurement (Gonçalves et al., 2020). For that, the films were cut in 3 x 3 cm squares, weighed, measured in diameter, and then immersed into 30 mL of distilled water (pH 6.5) containing sodium azide. The film specimens were left at room temperature (23 ± 2 °C) for 7 days in an orbital shaker at 80 rpm. After 7 days, all the non-solubilized remaining parts of the films were removed from the solution, weighed, and dried at 105 °C for 22 h. All the samples were then weighed to determine weight loss using equation (5).

$$\%Water\ solubility = \frac{w_b - w_a}{w_b} \times 100 \tag{5}$$

where w_b and w_a are the weights (g), without its residual humidity content determined by drying samples at 105 °C for 22 h) of the film before and after immersion into distilled water and drying, respectively.

The water swelling ratio was determined in triplicate by the films' dimensions change (Serra et al., 2015).

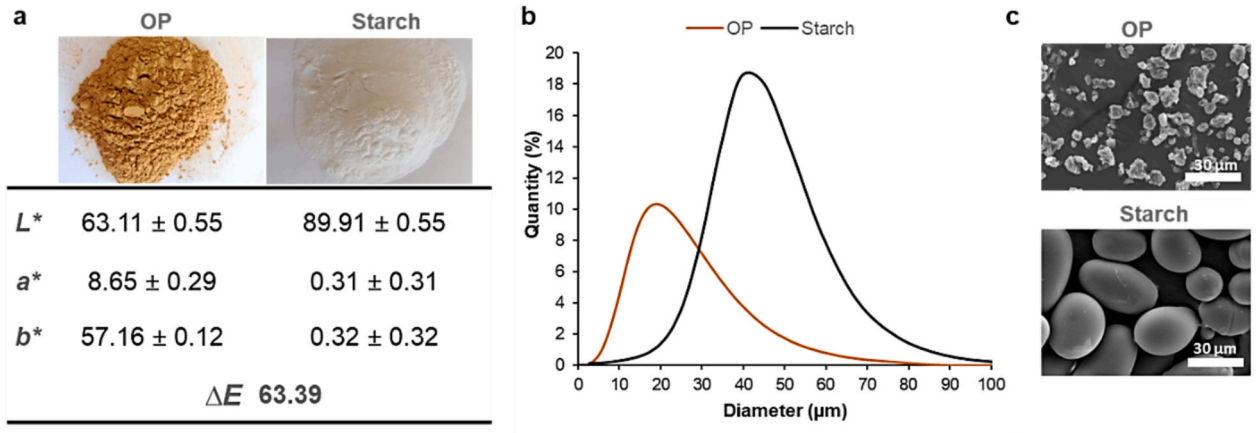

Fig. 1. Digital images and chromatic parameters **(a)**; Particle size distribution **(b)**; and SEM micrographs **(c)** of powdered onion peel (OP) and starch powders.

2.4.6. Antioxidant activity

The film's antioxidant activity measurement was designed to assess antioxidant performance in conditions that mimic real-life applications, where the active compounds remain embedded in the film matrix. As such, the ABTS assay was applied directly to film samples, enabling us to evaluate *in situ* antioxidant activity without requiring extraction. This experiment followed an adaptation of the 2.2′-azinobis-(3-ethylbenzothiazoline-6-sulfonic) acid (ABTS) method, as previously reported (Oliveira et al., 2020). Briefly, a 7 mM ABTS solution was prepared in aqueous potassium persulfate and kept in the dark at room temperature (23 °C ± 2 °C) for 12 h to ensure the $ABTS^{\cdot+}$ radical formation. Posteriorly, 1 mL of the $ABTS^{\cdot+}$ solution was diluted to obtain an absorbance between 0.700 and 0.850, measured at 734 nm in a BioTeK Synergy HT microplate reader (Vermont, EUA). Afterwards, film samples of 1 x 3 cm were placed in the diluted $ABTS^{\bullet+}$ solution at room temperature (23 °C ± 2 °C) under dark conditions. After each timepoint, the solutions absorbance was measured at 734 nm, using $ABTS^{\bullet+}$ solution without film as blank. Each experiment was carried out in triplicate for each developed formulation. The antioxidant activity was determined by the percentage of $ABTS^{\bullet+}$ inhibition calculated by Equation (6):

$$ABTS^{\cdot+}\,inhibition(\%) = \frac{A_b - A_f}{A_b} \times 100 \quad (6)$$

where A_b is the absorbance value (au) of the $ABTS^{\bullet+}$ solution without film (blank) and A_f is the absorbance value of the $ABTS^{\bullet+}$ solution exposed to the film sample.

2.5. Statistical analysis

All data obtained were statistically analyzed through one-way ANOVA tests, followed by a multiple comparison test (Tukey's HSD), using the GraphPad Prism version 5 for windows (trial version, GraphPad, USA). Significant differences were identified $p < 0.05$.

3. Results and discussion

The present study was undertaken with the objective of evaluating the feasibility of using powdered onion peel (OP) as an additive to mitigate the inherent hydrophilicity, water sensitivity, and gas permeability of cast starch-based films, while providing them with active properties. First, the characterization of powdered OP and recovered starch was performed. Then, the films were prepared incorporating different contents of powdered OP. The chromatic, morphological, mechanical, water resistance, gas barrier, and antioxidant properties of starch- and starch/OP films were determined and discussed considering their application as a packaging material.

3.1. Chromatic properties, particle size distribution, and morphology of powdered OP and starch

Regarding the chromatic properties (Fig. 1**a**), powdered OP showed an orange color with a L^* value of *ca.* 63.11, a very similar value to the one reported for brown onion powder (L^* value of *ca.* 64.50) (Jiang et al., 2020). However, a^* and b^* values of *ca.* 8.65 and *ca.* 57.16, respectively, were higher than those reported in literature (*ca.* 4.60 and *ca.* 14.00, respectively) (Jiang et al., 2020), tending to red more than green, and yellow more than blue. These differences can be related to the type of OP used, to the powdering conditions, and to the particle size distribution that can lead to distinct number of exposed pigments and lignocellulosic components, thus interfering with the final chromatic profile (Jiang et al., 2020).

The recovered starch presented a white color with a L^* of *ca.* 89.91, comparable to starch recovered by other authors from potato industry side streams (L^* value of *ca.* 91.55) (Singh et al., 2021). This byproduct showed a^* value of *ca.* 0.31, very close to the previously reported value of *ca.* 0.29 (Singh et al., 2021), and a b^* value of *ca.* 0.32, significantly lower that the previously reported values of *ca.* 1.58, meaning a more blueish tone, comparatively (Singh et al., 2021). It is important to note that recovered starches come from different natural sources that can lead to slightly different colorations.

Relatively to particle size distribution (Fig. 1**b**) and the morphology (Fig. 1**c**), powdered OP was constituted by irregularly shaped particles, a consequence of the ball milling process that disrupts the peel through flattening and fracturing into smaller and heterogenous pieces (Jiang et al., 2020) with an average size of *ca.* 20 μm, significantly lower than that reported for milled OP, showing a particle size diameter ranging higher than 132 μm. This effect is known to be dependent on the milling conditions, especially on milling time and velocity (Jiang et al., 2020).

Starch granules (Fig. 1**c**) had an oval and smooth shape and a medium size of *ca.* 38 μm, in accordance with previous studies (Gonçalves et al., 2020; Waterschoot et al., 2015). Taking in account that starch was recovered using sieving meshes between 90 μm and 150 μm, these results show that the sieving conditions promote agglomerates between starch granules.

3.2. Chemical composition of powdered OP and starch

The moisture content of powdered OP was *ca.* 8% (w/w related to dry OP weight), a much lower value than the one reported in literature for brown onion skin (*ca.* 52%) (El Mashad et al., 2019). This can be explained by the fact that the OP used in the present study has been already milled and subjected to a spray drying process, which can largely decrease its humidity content (Jiang et al., 2020).

From the chemical composition point of view, polysaccharides

Table 1
Chemical composition of powdered onion peel (OP).

	Content (% w/w OP weight)
Moisture	8.09 ± 0.01
Ethanol insoluble residue (AIR)	47.25 ± 0.00
from which *polysaccharides*	*64.80 ± 6.40*
Ethanol (80% V/V) soluble compounds (ASM)	11.81 ± 0.00
from which carb*ohydrates*	*34.89 ± 2.53*
Lipids	5.92 ± 0.00
from which *oils*	*5.27 ± 1.40*
from which *chloroform soluble waxes*	*0.65 ± 0.12*
Phenolics (GAE)	4.70 ± 0.05
Protein	2.21 ± 0.01
Ashes	27.23 ± 5.98

accounted for 64.80% of the ethanol-insoluble residue (AIR) fraction (Table 1), with AIR constituting 47.25% of the total OP composition. Based on this, the absolute polysaccharide content in OP was approximately 31% (w/w related to dry OP weight), calculated as 64.80% of the 47.25% AIR fraction. AIR was majorly constituted by uronic acids (*ca.* 60%), glucose (*ca.* 33%), and residual amounts of xylose (*ca.* 2%), mannose (*ca.* 1%), and galactose (*ca.* 1%) (Fig. 2). This composition suggests the presence of pectic polysaccharides together with cellulose, typical of the onion brown outer skin (Benito-Román et al., 2022).

It was possible to observe that the soluble compounds in 80% v/v ethanol (ASM) also contained carbohydrates. This fraction contained major glucose (*ca.* 79%) and residual amounts of arabinose (*ca.* 7%), uronic acids (*ca.* 5%), mannose (*ca.* 3%), galactose (*ca.* 2%), rhamnose (*ca.* 2%), and xylose (*ca.* 1%) (Fig. 2). These results are in accordance with previous results for outer brown onion peel (Choi et al., 2015; Putnik et al., 2019). A possible source of glucose in the ASM fraction of OP is its phenolic compounds, usually rich in glucose, as shown by the detection of GAE in Table 1 (Ali et al., 2016; Boo et al., 2012; Ko et al., 2011; Munir et al., 2018).

The amount of protein (Table 1) determined in powdered OP was *ca.* 2% (w/w related to dry OP weight). The lipids solubilized from powdered OP accounted for *ca.* 5% correspond to the oil and *ca.* 1% to the waxes. As the methodology used to extract waxes did not use a saponification step, it is possible that most of the waxes remained in OP (Nuissier et al., n.d). The amount of total phenolics detected in powdered OP expressed by GAE was *ca.* 5% (w/w related to dry OP weight). These compounds could possibly correspond to the flavonoids and anthocyanins (Ali et al., 2016; Boo et al., 2012; Ko et al., 2011; Munir et al., 2018). Inorganic matter was also detected in the powdered OP, as observed by the formation of *ca.* 27% ashes, which indicates the presence of minerals in OP, corroborating with the potassium, calcium, magnesium, iron, zinc, manganese, and selenium reported for onion peels (El Mashad et al., 2019). Nonetheless, the sum of the individual components slightly exceeds 100 percent, likely due to overlapping fraction assignments, where compounds such as phenolics, proteins, or minerals may be distributed across multiple fractions, including AIR and ASM, and were quantified independently. Regarding the chemical composition of starch recovered from potato washing slurries, it contained *ca.* 8% (w/w related to dry starch weight) moisture and *ca.* 65% starch (w/w related to dry starch weight) (Table 2), in accordance with previously reported values (Gonçalves et al., 2020).

The recovered starch contained *ca.* 0.46% of protein, like the 0.3% detected in starch recovered from potato (Alvani et al., 2011). The ashes content on this starch was almost inexistant (*ca.* 0.06%).

The amylose and amylopectin detected in this starch was of *ca.* 44.9% and 55.1%, respectively. A higher amylopectin content is expected, as this trend is commonly reported for potato starch (Gonçalves et al., 2020). However, the amylopectin/amylose ratio of 1.2 is a lower

Table 2
Chemical composition and gelatinization properties of starch recovered from potato washing slurries.

	Recovered starch
Moisture (% weight loss)	8.35 ± 0.42
Starch content (wt.% in dry matter)	64.99 ± 1.98
Amylose (wt.%)	44.90 ± 2.06
Amylopectin (wt.%)	55.09 ± 1.45
Protein (wt.%)	0.46 ± 0.01
Ashes (wt.%)	0.06 ± 0.00
Gelatinization temperatures and enthalpy	
T_0 (°C)	60.59 ± 0.31
T_p (°C)	64.99 ± 1.98
T_c (°C)	745 ± 0.01
ΔH (J/g)	3.1 ± 0.2

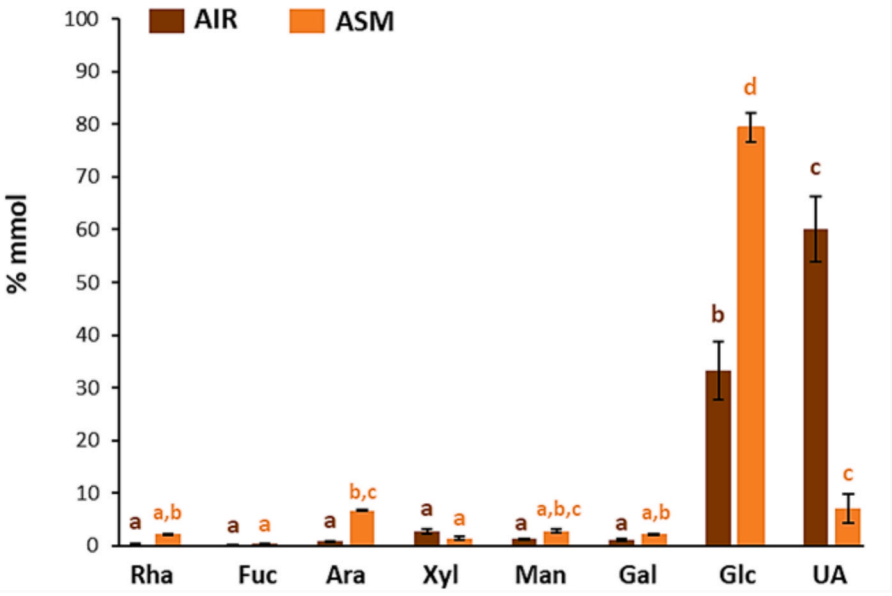

Fig. 2. Carbohydrate composition (% mmol) of alcohol insoluble residue (AIR) and alcohol soluble matter (ASM) derived from powdered onion peel. Different letters indicate significant differences ($p < 0.05$). Rha: rhamnose, Fuc: Fucose, Ara: Arabinose, Xyl: Xylose, Man: Mannose, Gal: Galactose, UA: Uronic acids.

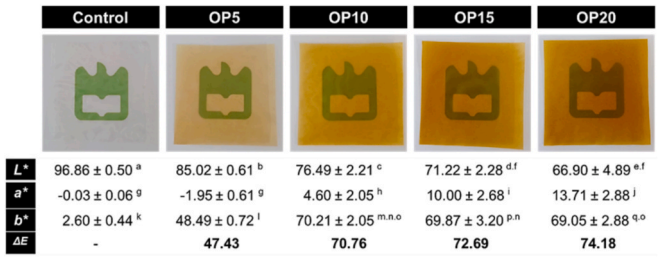

Fig. 3. Digital images and chromatic properties of starch-based films without (Control) and with 5 wt% (OP5), 10 wt% (OP10), 15 wt% OP (OP15) and 20 wt % onion peel (OP20): L^* (luminosity), a^* (red/green color), b^* (yellow/blue color), and total difference in color (ΔE) regarding the control. Different letters indicate significant differences ($p < 0.05$).

than previously reported values of 2.3 for this starch (Gonçalves et al., 2020), indicating that this sample can be classified as a high-amylose, low-waxy starch (Tester et al., 2004).

When analyzing the differential scanning calorimetry thermogram of the recovered starch (Supplementary Fig. S1), the onset temperature (T_o) was *ca.* 60 °C, corresponding to starch granule hydration; the peak temperature (T_p) was *ca.* 66 °C, attributed to the reorganization of amylose and amylopectin chains; and the conclusion temperature (T_c) was *ca.* 75 °C, marking the completion of gelatinization (Gonçalves et al., 2020) (Table 2).These values align with previous reports for potato starch (T_o: 58.7–62.5 °C, T_p: 62.5–66.1 °C, T_c: 67.3–72.3 °C) (Alvani et al., 2011). However, the gelatinization enthalpy (ΔH) of *ca.* 3.1 J/g was significantly lower than previously reported values for potato starch (15.1–18.4 J/g), indicating that less hydrogen bond disruption inside the granule was required for gelatinization, suggesting a lower degree of molecular order (Alvani et al., 2011).

3.3. Characterization of starch- and starch/OP-based films

3.3.1. Chromatic properties

From the chromatic point of view (Fig. 3), colorless and transparent starch-based films presented a luminosity (L^*) value of *ca.* 96.86 and red/green (a^*) and yellow/blue (b^*) coordinates of *ca.* −*0.03* and *ca.* 2.6, respectively. In the presence of OP, they gained an orangish coloration, maintain their transparency, acquiring L^*, a^*, and b^* coordinates ranging from *ca.* 85.02 to 66.9, −1.95 to 13.71, and 48.49 to 69.05, respectively. These chromatic changes varied directly with the OP amount, as verified by the ΔE values. The leaching of OP's hot-water soluble pigments, such as anthocyanins and carotenoids (Bello et al., 2013; Boo et al., 2012; Munir et al., 2018; Putnik et al., 2019) during the starch gelatinization process justifies the orangish coloration that OP conferred to the starch-based films.

3.3.2. Morphology

As a consequence of the solvent casting process, the surface of starch-based films that remained in direct contact with the plexiglass plate (bottom) was highly smooth, shaping the surface of the support material, whereas the surface exposed to the air (top) during casting showed a hill-valley-structure (Fig. 4), which could be promoted by the water molecules evaporation (Gonçalves et al., 2020). When incorporated into starch-based formulation, the powdered OP conferred heterogeneity to both bottom and top surfaces, with OP particles mostly accumulated onto the top surface. Although OP is denser than starch, as shown in previous studies (Karthikeyan, 2021; Manek et al., 2012), this distribution is primarily driven by solvent evaporation dynamics, phase separation, and particle–matrix interactions rather than gravity. As water evaporates, upward convective flow transports OP particles toward the air interface, particularly larger and less soluble fractions. Additionally, OP's high fiber and lipid content increase its affinity for the polymer-air interface, reducing sedimentation. Similar migration effects have been reported in starch-based films incorporating fibrous by-products such as coffee silverskin (Oliveira et al., 2020) and pomegranate peel (Ali et al., 2019), further supporting the role of convective transport and polymer interactions over density-driven settling. As OP particles were dragged onto the films surface, a greater degree of heterogeneity was observed, directly related to OP dosage. This effect is to be also visible in the cross-section micrographs, where the control presents a smooth, homogeneous, and regular interior, whereas OP-doped

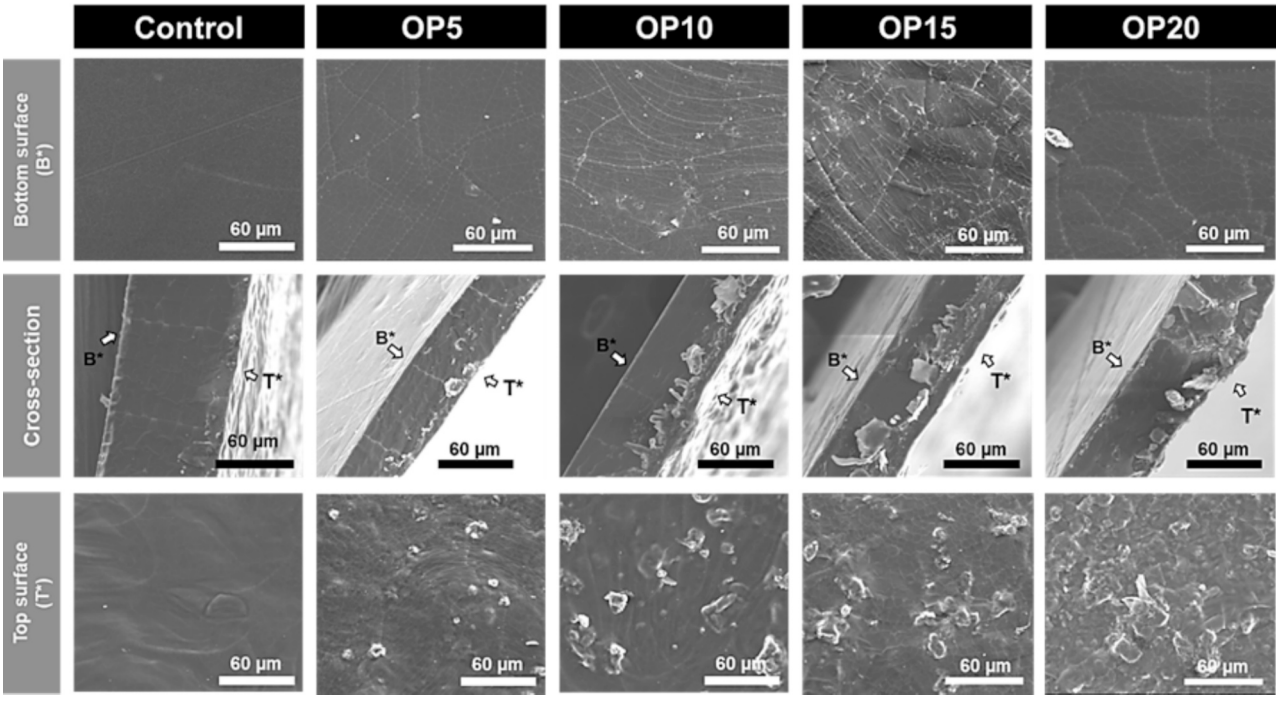

Fig. 4. SEM micrographs of the bottom, cross-section, and top surfaces of starch-based films without (Control) and with 5 wt% (OP5), 10 wt% (OP10), 15 wt% OP (OP15) and 20 wt% OP (OP20).

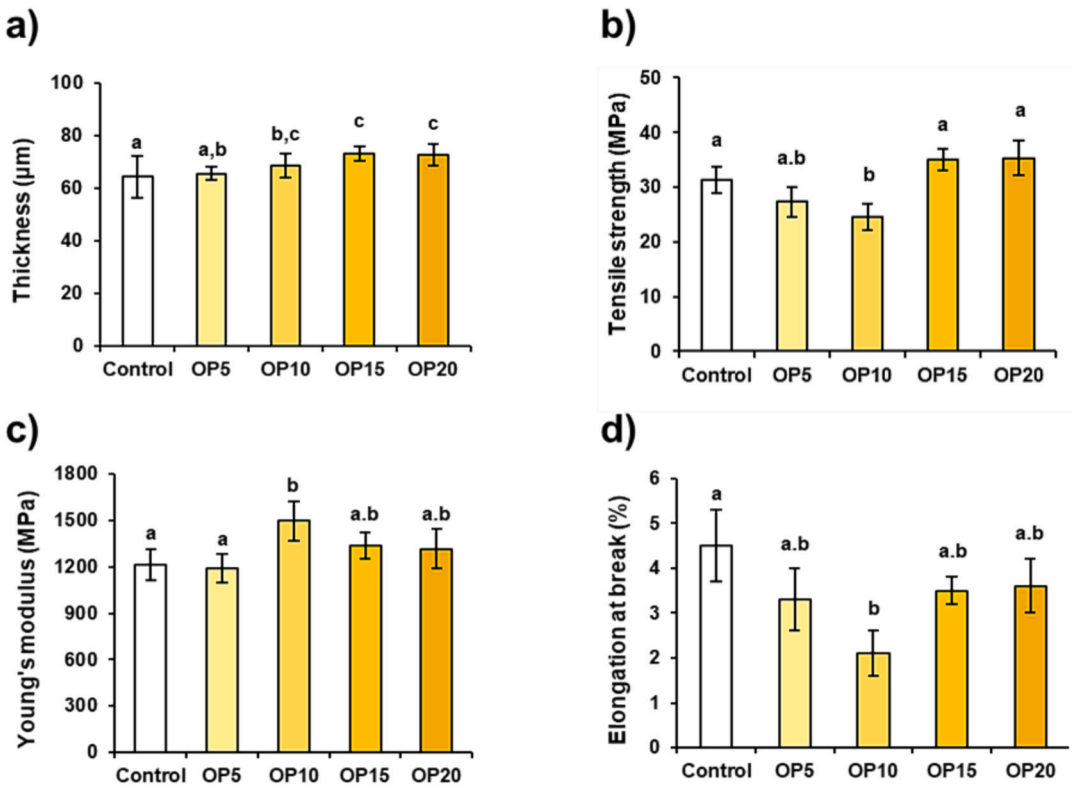

Fig. 5. Thickness (**a**), tensile strength (**b**), Youngs modulus (**c**), and elongation at break (**d**) of starch-based films without (Control) and with 5 wt% (OP5), 10 wt% (OP10), 15 wt% OP (OP15) and 20 wt% OP (OP20). Different letters indicate significant differences ($p < 0.05$).

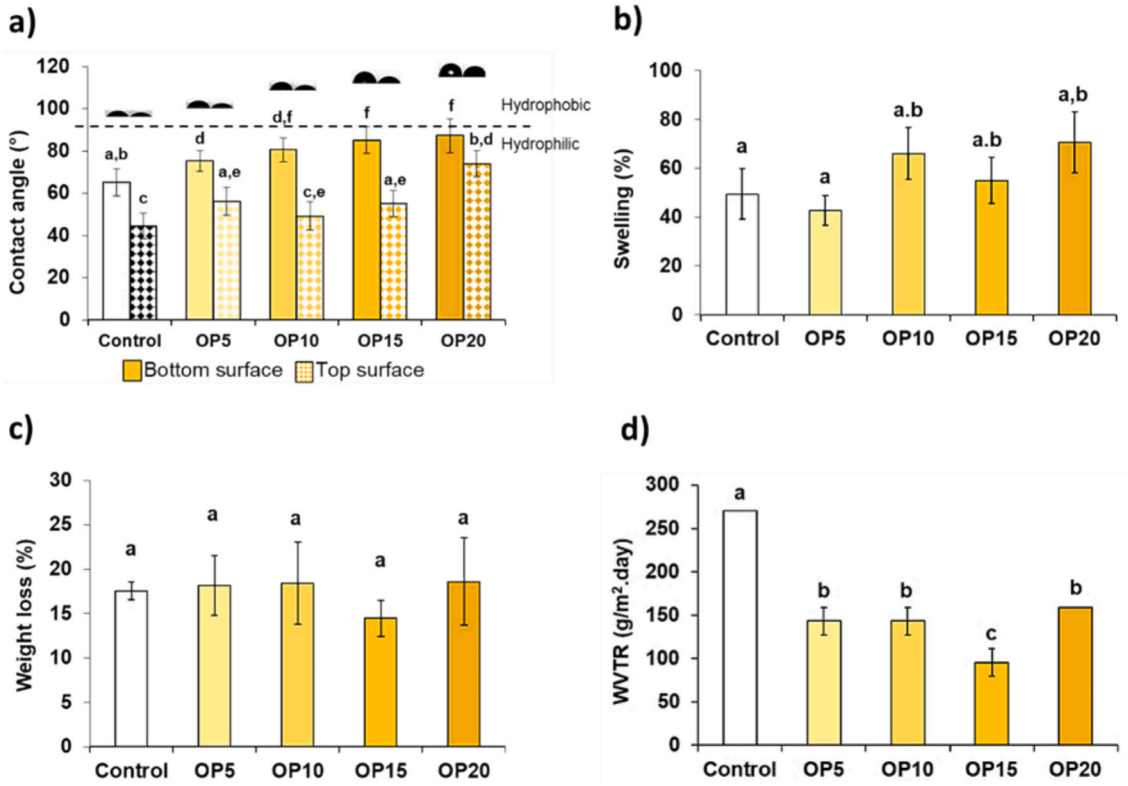

Fig. 6. Water contact angle values (a) established between a ultrapure water drop and the bottom (full color) and top (doted color) surfaces of starch-based films without (Control) and with 5 wt% (OP5), 10 wt% (OP10), 15 wt% OP (OP15), and 20 wt% OP (OP20); Water swelling (b) and solubility (b) of starch-based films without (control) and with 5 wt% (OP5), 10 wt% (OP10), 15 wt% OP (OP15) and 20 wt% OP (OP20); Water vapor transmission rate (d) of starch-based films without (control) and with 5 wt% (OP5), 10 wt% (OP10), 15 wt% OP (OP15) and 20 wt% OP (OP20). Different letters indicate significant differences ($p < 0.05$).

films show a clear accumulation of particles on the top surface.

3.3.3. Thickness and mechanical performance

Starch-based films had a thickness of *ca.* 64 μm. When 5 wt% OP was incorporated, their thickness did not significantly change (Fig. 5), contrarywise to the use of higher OP content that increased the films' thickness up to *ca.* 73 μm. This result is mostly related to an increase in OP content (w/w dry starch weigh), which led to an increase in the total mass content within the same area of film, and a reduction in the amount of water needed to evaporate, thus leading to a thicker film.

Considering the mechanical performance, starch-based films exhibited a tensile strength of *ca* 31.4 MPa, a Youngs modulus of *ca.* 1214 MPa, and an elongation at break of *ca.* 5%. This performance remained statistically unchanged except for samples containing 10 wt% OP, where tensile strength and elongation at break decreased to *ca.* 25 MPa and *ca.* 2%, respectively, while Young's modulus increased to *ca.* 1496 MPa, indicating enhanced rigidity. This change suggests that, at 10 wt%, particles effectively fill the free hydrodynamic volume within the starch matrix, interacting with amylose, amylopectin, glycerol, and OP-derived hot-water-solubilized compounds (such as carbohydrates and phenolic compounds). As a result, OP acts as a reinforcing filler, increasing film stiffness. Similar trends have been reported in starch-based films containing 10% pomegranate peel, where increased rigidity was observed due to effective matrix reinforcement (Ali et al., 2019). However, at higher OP concentrations (≥15 wt%), rigidity enhancement is compromised. This can be attributed to the increased release of OP-derived water-soluble biomolecules during starch gelatinization, which, similar to glycerol, exhibit plasticizing effects and counteract the stiffness imparted by OP. A comparable behaviour was observed in starch-based films incorporating coffee silverskin, where rigidity increased up to 15% subproduct content, followed by a decline at higher concentrations (Oliveira et al., 2020). From these results, it can be concluded that at low OP concentrations (≤10 wt%), OP's fibrous polysaccharides integrate well with starch, enhancing rigidity and increasing Young's modulus. However, at higher OP concentrations (≥15 wt%), excessive OP creates phase discontinuities and weak interfacial adhesion, reducing stress transfer efficiency and leading to lower tensile strength and elongation at break. Additionally, SEM micrographs confirm these structural changes (Fig. 4), reinforcing the proposed mechanisms.

3.3.4. Water wettability, swelling, and solubility

Regarding the water wettability (Fig. 6 **a-c**), when dispersed onto starch-based films, the ultrapure water drops originated contact angles between the bottom and top samples' surfaces of *ca.* 44° and *ca.* 65°, respectively, highlighting their heterogeneity. These values evidence the hydrophilic profile of starch-based films, a consequence of the high amount of hydroxyl groups available in the starch polymeric structure (Oliveira et al., 2020). The lower water tolerance given by the lowest water contact angle observed on the films' top surfaces can be related with the diffusion of water-soluble and low-density molecules, such as glycerol and residual low molecular weight carbohydrates present in the recovered starch (Table 2) during the drying process (Gonçalves et al., 2020; Shabir et al., 2022).

In the presence of OP, regarding to the top surface, water contact angle increased up to *ca.* 74°, bringing it closer to the hydrophobicity benchmark (90°), except for starch/10% OP-based films that remained like the control sample. Relatively to the bottom surface, water contact angle increased up to 87°, a much closer value to the hydrophobicity benchmark. Therefore, OP increased the water tolerance of starch-based films. This behaviour can be derived from the OP's hot-water extractable molecules (such as lipids and phenolic compounds) that hinder the availability for starch polymers interacting with water molecules (Gonçalves et al., 2021)(Ali et al., 2019). However, this feature was jeopardized using 10% OP, a consequence that may derive from the highest rigidity of starch/10% OP-based films that difficult the water

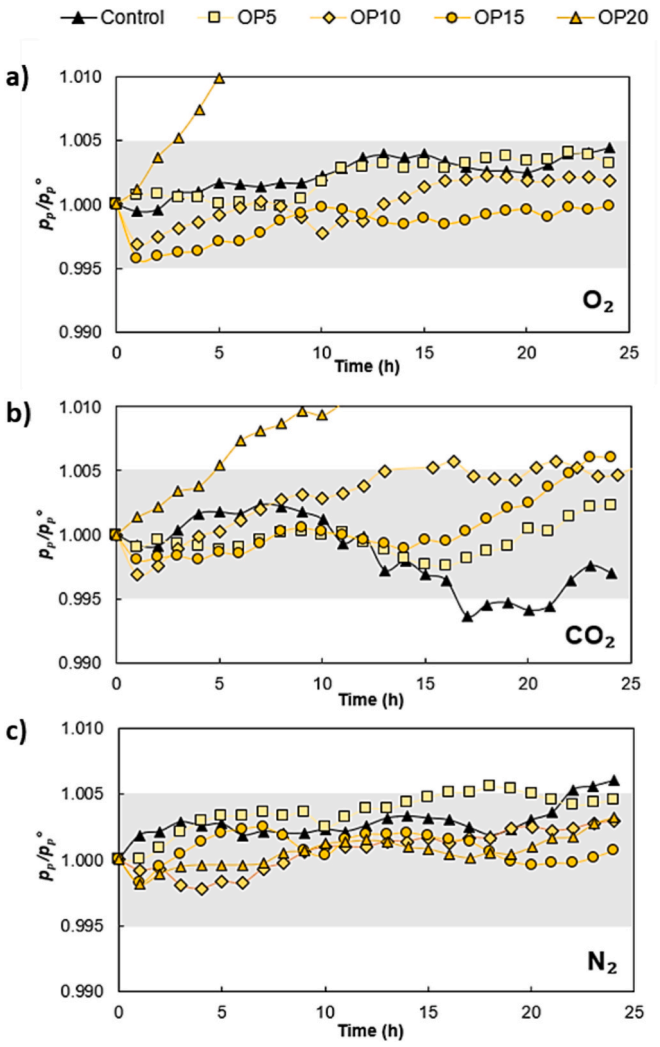

Fig. 7. Normalized permeate pressure of starch-based films without (Control) and with 5 wt% (OP5), 10 wt% (OP10), 15 wt% OP (OP15) and 20 wt% onion peel (OP20) to (**a**) oxygen, (**b**) carbon dioxide, and (**c**) nitrogen. Expanded uncertainty is represented by the shaded part of the graphic.

wettability of starch polymers (Gonçalves et al., 2021, 2020; Ko et al., 2011; Munir et al., 2018).

When immersed into water, starch- and starch/OP-based films showed a swelling and solubility ranging from *ca.* 43–71% and *ca.* 13–19%, respectively (Fig. 6 **b,c**), but without statistical significance. Therefore, although OP increased the water wettability of starch-based films, it did not significantly change the water swelling and solubility of the films. A similar behaviour was observed in starch-based films loaded with genipin, where an increase in the films water contact angle has been observed, with no changes in their swelling or solubility (Gonçalves et al., 2021). This behaviour can be explained by the interactions between starch molecules and the proteins/polysaccharides within OP, which, in combination with disrupted starch granules, created a cohesive structure. Such organization prevented the swelling of the films, which avoided the glycerol migration to the aqueous medium, leading to a bigger resistance of the films to solubilization (Gonçalves et al., 2021).

3.3.5. Barrier properties

Concerning the water vapor transmission rate (WVTR) (Fig. 6**d**), starch-based films showed an average value of 270 g/(m^2.day), corroborating with a previously reported value (Petronilho et al., 2021). The incorporation of OP significantly decreased the films' WVTR,

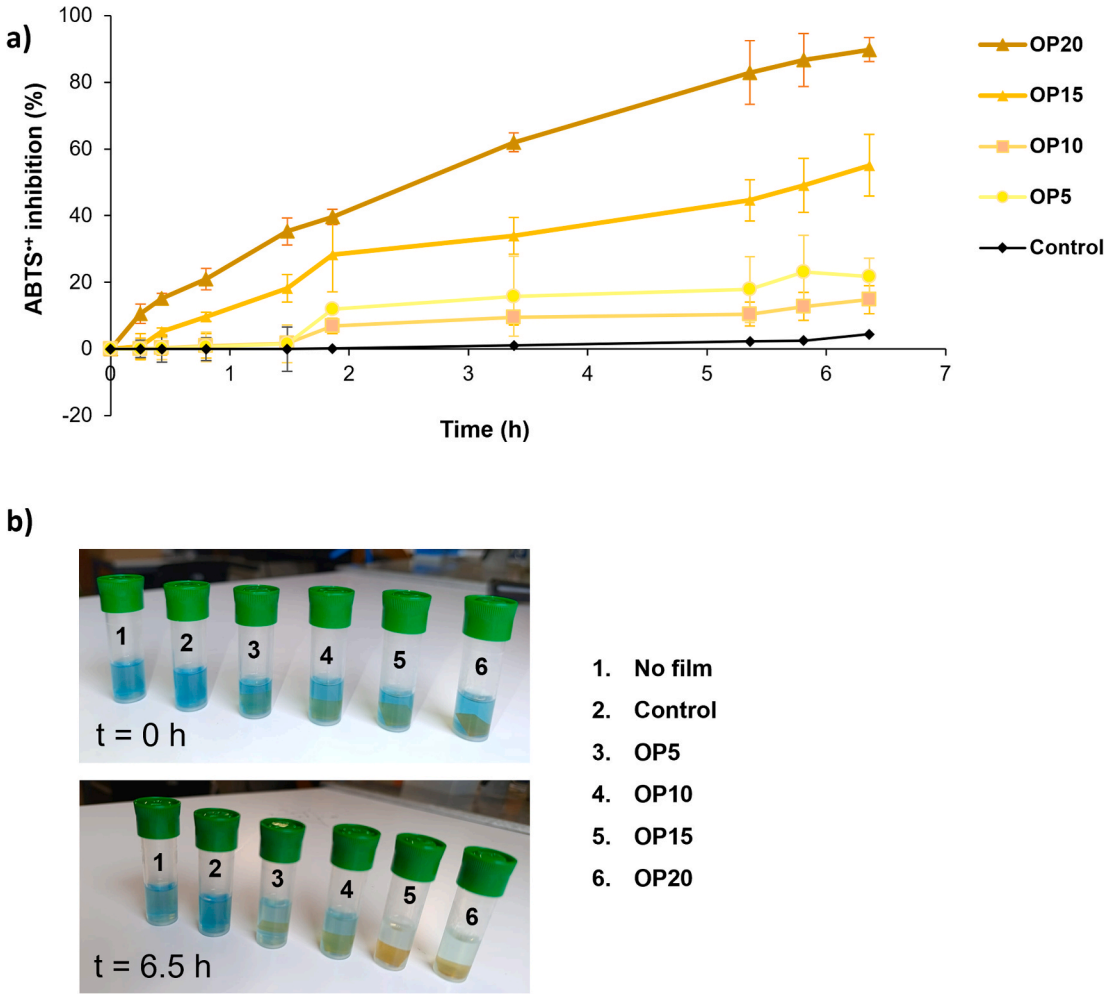

Fig. 8. a) Percentage of $ABTS^{\bullet+}$ inhibition of starch-based films without OP (Control) and with 5 wt% (OP5), 10 wt% (OP10), 15 wt% OP (OP15) and 20 wt% onion peel (OP20) during 6.5 h of incubation. Different letters represent values that are significantly different ($p < 0.05$); **b)** Digital images of $ABTS^{\bullet+}$ solution with no film and submersing the starch-based films without OP (Control) and with 5 wt% (OP5), 10% (OP10), 15 wt% OP (OP15) and 20 wt% onion peel (OP20), after timepoints 0 h and 6.5 h.

reaching the lowest value of 95 g/(m^2.day) when 15 wt% OP was used. This decrease resulted from the hot-water soluble OP-derived compounds released during the compounding that engage hydrogen bonding with starch polymers, hindering their interaction with water molecules (Singh et al., 2022) (Table 2), and the presence of intact OP particles in the polymeric matrix that promote a tortuous pathway for the water molecules, forming a natural physical barrier against water molecules (Fig. 4).

Regarding the O_2, CO_2, and N_2 permeability, Fig. 7 illustrates the normalized permeate pressure observed throughout the experiment. As shown, starch-based films had a barrier behaviour to all the gases throughout 24 h, since no permeation was observed. This conclusion is supported by the fact that the permeate pressure remained within the expanded uncertainty interval, represented by the shaded region in the figure.

Compared to the neat films OP incorporation did not significantly alter the gas permeability of starch-based films up to 15 wt% OP, since the permeate pressure over time remained within the expanded uncertainty interval for these compositions. However, at 20 wt% OP, oxygen permeability increased to 43 Barrer, which remains within the range of acceptable values for biopolymer-based food packaging applications (Bao et al., 2006; Michiels et al., 2017). The increase in oxygen permeability at 20 wt% OP is attributed to microstructural modifications, where excess OP may introduce discontinuities in the polymer matrix, leading to higher diffusivity of oxygen molecules as it is demonstrated in Fig. 4 (Shafiq et al., 2021). Furthermore, the presence of OP particle agglomerates in the polymeric matrix could lead to the formation of interfacial voids, which may serve as preferential pathways for gas molecules (Wolf et al., 2018). Despite this increase, the measured permeability values remain lower than those reported for other polysaccharide-based films used in food preservation (Zabihzadeh Khajavi et al., 2020). Thus, starch/OP-based films retain their potential as functional barrier materials, while also providing additional antioxidant benefits, making them suitable for biodegradable and active packaging applications. Furthermore, the presence of OP particle agglomerates in the polymeric matrix could also lead to the formation of interfacial voids, which may serve as preferential pathways for gas molecules (Bao et al., 2006; Michiels et al., 2017; Wolf et al., 2018).

3.3.6. *Antioxidant activity*

The antioxidant activity of starch-based films was assessed through ABTS•+ inhibition over 6.5 h, as shown in Fig. 8. Films without onion peel (OP) (control) exhibited minimal $ABTS^{\bullet+}$ inhibition (*ca.* 4%), maintaining the blueish coloration of the $ABTS^{\bullet+}$ solution throughout the exposure period. This slight antioxidant activity is attributed to the presence of phenolic compounds naturally occurring in non-purified potato starch used for film preparation (Lopes et al., 2021).

Incorporating OP significantly enhanced the antioxidant activity of

the films, with inhibition increasing proportionally to OP content. Starch/20 wt% OP-based films demonstrated the highest $ABTS^{\bullet+}$ inhibition (*ca.* 90%) after 6.5 h, leading to an almost complete disappearance of the blue coloration, indicating extensive $ABTS^{\bullet+}$ radical scavenging. This improvement is attributed to the presence of OP-derived phenolic compounds, including anthocyanins, carotenoids, and quercetin, which are recognized for their strong antioxidant properties (Chadorshabi et al., 2022; El Mashad et al., 2019). The antioxidant response followed an increasing trend with OP content, except for the starch/10 wt% OP-based films, which exhibited lower inhibition levels, like the 5 wt% OP films. This deviation can be explained by the higher rigidity of starch/10 wt% OP-based films (Fig. 5**c**), which may have restricted the molecular mobility of antioxidant compounds within the polymeric network, limiting their interaction with $ABTS^{\bullet+}$ radicals.

4. Conclusions

This study demonstrates the potential of directly incorporating powdered onion peel (OP) into starch-based films as a sustainable waste valorization strategy. By eliminating extraction steps and fully utilizing OP, this approach aligns with circular economy principles, enhancing bioplastic properties while reducing agro-industrial waste. Due to its composition, OP acts as both a plasticizer and filler, improving barrier properties against water vapor and gases (O_2, CO_2, N_2) up to 15 wt% while maintaining wettability, rigidity, transparency, and antioxidant activity. With 1.6 g of OP yielding 864 cm^2 of bioplastic, the 550,000 tons of wasted OP annually could generate approximately 27,000 km^2 of bio-based films. However, scaling up remains a challenge due to the solvent casting method. Optimizing lab-to-industry transition could enhance feasibility, maximize OP incorporation and further improve material performance. Beyond OP, this approach provides a scalable model for repurposing other agro-industrial byproducts, reinforcing the role of waste-derived bioplastics in circular economy strategies.

CRediT authorship contribution statement

Mariana Vallejo: Writing – original draft, Methodology, Investigation, Data curation. **Beatriz Esteves:** Writing – review & editing, Methodology, Data curation. **Pedro Carvalho:** Writing – review & editing, Methodology, Data curation. **Manuel A. Coimbra:** Writing – review & editing, Conceptualization. **Martinho Oliveira:** Writing – review & editing, Validation, Supervision. **Paula Ferreira:** Writing – review & editing, Validation, Supervision. **Idalina Gonçalves:** Writing – review & editing, Validation, Supervision, Conceptualization.

Declaration of competing interest

The authors declare that they have no known competing financial interests or personal relationships that could have appeared to influence the work reported in this paper.

Acknowledgements

The authors would like to thank to University of Aveiro and FCT/MCES for the financial support from CICECO - Institute of Materials of Aveiro (UIDB/50011/2020 (DOI 10.54499/UIDB/50011/2020), UIDP/50011/2020 (DOI 10.54499/UIDP/50011/2020) & LA/P/0006/2020 (DOI 10.54499/LA/P/0006/2020)) and LAQV-REQUIMTE (UIDB/50006/2020; UIDP/50006/2020) through PT national funds. FCT is also thanked for funding a PhD grant (MV, 2022.13787.BD) and the Individual Call to Scientific Employment Stimulus (IG, https://doi.org/10.54499/CEECIND/00430/2017/CP1459/CT0032). The authors also thank to the Portuguese companies CALCOB and A Saloinha, Lda. for providing onion peels and starch-rich potato washing slurries, respectively.

Appendix A. Supplementary data

Supplementary data to this article can be found online at https://doi.org/10.1016/j.wasman.2025.115005.

Data availability

Data will be made available on request.

References

Pamula, A.S.P., Hung, Y.-T., Paul, H.-C., 2021. Utilization of Agro-based Adsorbents in Binary Wastewater Treatment. Journal of Environmental Science and Pollution Research 7, 451–454. https://doi.org/10.30799/jespr.213.21070103.

Ali, A., Chen, Y., Liu, H., Yu, L., Baloch, Z., Khalid, S., Zhu, J., Chen, L., 2019. Starch-based antimicrobial films functionalized by pomegranate peel. Int. J. Biol. Macromol. 129, 1120–1126. https://doi.org/10.1016/j.ijbiomac.2018.09.068.

Ali, O.-H., Al-sayed, H., Yasin, N., Afifi, E., 2016. Effect of Different Extraction Methods on Stablity of Anthocyanins Extracted from Red Onion peels (Allium cepa) and its Uses as Food Colorants. Bulletin of the National Nutrition Institute 47, 1–24. https://doi.org/10.21608/bnni.2016.4218.

Alvani, K., Qi, X., Tester, R.F., Snape, C.E., 2011. Physico-chemical properties of potato starches. Food Chem. 125, 958–965. https://doi.org/10.1016/j.foodchem.2010.09.088.

Bao, L., Dorgan, J.R., Knauss, D., Hait, S., Oliveira, N.S., Maruccho, I.M., 2006. Gas permeation properties of poly(lactic acid) revisited. J Memb Sci 285, 166–172. https://doi.org/10.1016/j.memsci.2006.08.021.

Bello, M., Olabanji, I.O., Abdul-Hammed, M., 2013. Characterization of domestic onion wastes and bulb (Allium cepa L.): Fatty acids and Metal Contents, Article. Int. Food Res. J.

Benito-Román, O., Alonso-Riaño, P., Díaz De Cerio, E., Sanz, M.T., Beltrán, S., 2022. Semi-continuous hydrolysis of onion skin wastes with subcritical water: Pectin recovery and oligomers identification. J. Environ. Chem. Eng. 10. https://doi.org/10.1016/j.jece.2022.107439.

Berenguer, C.V., Andrade, C., Pereira, J.A.M., Perestrelo, R., Câmara, J.S., 2023. Current challenges in the Sustainable Valorisation of Agri-Food Wastes: a Review. Processes. https://doi.org/10.3390/pr11010020.

Bhargava, N., Sharanagat, V.S., Mor, R.S., Kumar, K., 2020. Active and intelligent biodegradable packaging films using food and food waste-derived bioactive compounds: a review. Trends Food Sci. Technol. https://doi.org/10.1016/j.tifs.2020.09.015.

Boccalon, E., Viscusi, G., Lamberti, E., Fancello, F., Zara, S., Sassi, P., Marinozzi, M., Nocchetti, M., Gorrasi, G., 2022. Composite films containing red onion skin extract as intelligent pH indicators for food packaging. Appl. Surf. Sci. 593. https://doi.org/10.1016/j.apsusc.2022.153319.

Boo, H.O., Hwang, S.J., Bae, C.S., Park, S.H., Heo, B.G., Gorinstein, S., 2012. Extraction and characterization of some natural plant pigments. Ind. Crops Prod. 40, 129–135. https://doi.org/10.1016/j.indcrop.2012.02.042.

Chadorshabi, S., Hallaj-Nezhadi, S., Ghasempour, Z., 2022. Red onion skin active ingredients, extraction and biological properties for functional food applications. Food Chem. https://doi.org/10.1016/j.foodchem.2022.132737.

Choi, I.S., Cho, E.J., Moon, J.H., Bae, H.J., 2015. Onion skin waste as a valorization resource for the by-products quercetin and biosugar. Food Chem. 188, 537–542. https://doi.org/10.1016/j.foodchem.2015.05.028.

El Mashad, H.M., Zhang, R., Pan, Z., 2019. Onion and Garlic, in: Integrated Processing Technologies for Food and Agricultural By-Products. Elsevier, pp. 273–296. Doi: 10.1016/B978-0-12-814138-0.00011-3.

Fernandes, P.A.R., Ferreira, S.S., Bastos, R., Ferreira, I., Cruz, M.T., Pinto, A., Coelho, E., Passos, C.P., Coimbra, M.A., Cardoso, S.M., Wessel, D.F., 2019. Apple pomace extract as a sustainable food ingredient. Antioxidants 8. https://doi.org/10.3390/antiox8060189.

Fraga, S.C., Monteleone, M., Lanč, M., Esposito, E., Fuoco, A., Giorno, L., Pilnáček, K., Friess, K., Carta, M., McKeown, N.B., Izák, P., Petrusová, Z., Crespo, J.G., Brazinha, C., Jansen, J.C., 2018. A novel time lag method for the analysis of mixed gas diffusion in polymeric membranes by on-line mass spectrometry: Method development and validation. J Memb Sci 561, 39–58. https://doi.org/10.1016/j.memsci.2018.04.029.

Gonçalves, I., Hernández, D., Cruz, C., Lopes, J., Barra, A., Nunes, C., da Silva, J.A.L., Ferreira, P., Coimbra, M.A., 2021. Relevance of genipin networking on rheological, physical, and mechanical properties of starch-based formulations. Carbohydr. Polym. 254. https://doi.org/10.1016/j.carbpol.2020.117236.

Gonçalves, I., Lopes, J., Barra, A., Hernández, D., Nunes, C., Kapusniak, K., Kapusniak, J., Evtyugin, D.V., Lopes da Silva, J.A., Ferreira, P., Coimbra, M.A., 2020. Tailoring the surface properties and flexibility of starch-based films using oil and waxes recovered from potato chips byproducts. Int. J. Biol. Macromol. 163, 251–259. https://doi.org/10.1016/j.ijbiomac.2020.06.231.

Gulati, M., Keshav, K.M., Reddy, J.P., 2023. Effect of Onion Peel Extract on Structural, Mechanical, thermal, and Antioxidant Properties of Methylcellulose Films. Food Bioproc. Tech. 16, 2328–2342. https://doi.org/10.1007/s11947-023-03054-9.

Jiang, G., Ramachandraiah, K., Wu, Z., Li, S., Eun, J.B., 2020. Impact of ball-milling time on the physical properties, bioactive compounds, and structural characteristics of onion peel powder. Food Biosci. 36. https://doi.org/10.1016/j.fbio.2020.100630.

Karthikeyan, S., 2021. Strengthening of Black Cotton Soil Against Liquefaction using Onion Peel.

Ko, M.J., Cheigh, C.I., Cho, S.W., Chung, M.S., 2011. Subcritical water extraction of flavonol quercetin from onion skin. J. Food Eng. 102, 327–333. https://doi.org/10.1016/j.jfoodeng.2010.09.008.

Kumar, M., Barbhai, M.D., Hasan, M., Punia, S., Dhumal, S., Radha, Rais, N., Chandran, D., Pandiselvam, R., Kothakota, A., Tomar, M., Satankar, V., Senapathy, M., Anitha, T., Dey, A., Sayed, A.A.S., Gadallah, F.M., Amarowicz, R., Mekhemar, M., 2022. Onion (Allium cepa L.) peels: A review on bioactive compounds and biomedical activities. Biomedicine and Pharmacotherapy. Doi: 10.1016/j.biopha.2021.112498.

Liang, T., Sun, G., Cao, L., Li, J., Wang, L., 2018. Rheological behavior of film-forming solutions and film properties from Artemisia sphaerocephala Krasch. gum and purple onion peel extract. Food Hydrocoll. 82, 124–134. https://doi.org/10.1016/j.foodhyd.2018.03.055.

Lopes, J., Gonçalves, I., Nunes, C., Teixeira, B., Mendes, R., Ferreira, P., Coimbra, M.A., 2021. Potato peel phenolics as additives for developing active starch-based films with potential to pack smoked fish fillets. Food Packag. Shelf Life 28. https://doi.org/10.1016/j.fpsl.2021.100644.

Manek, R.V., Builders, P.F., Kolling, W.M., Emeje, M., Kunle, O.O., 2012. Physicochemical and binder properties of starch obtained from Cyperus esculentus. AAPS PharmSciTech 13, 379–388. https://doi.org/10.1208/s12249-012-9761-z.

Michalak-Majewska, M., Teterycz, D., Muszyński, S., Radzki, W., Sykut-Domańska, E., 2020. Influence of onion skin powder on nutritional and quality attributes of wheat pasta. PLoS One 15. https://doi.org/10.1371/journal.pone.0227942.

Michiels, Y., Van Puyvelde, P., Sels, B., 2017. Barriers and chemistry in a bottle: Mechanisms in today's oxygen barriers for tomorrow's materials. Applied Sciences (switzerland). https://doi.org/10.3390/app7070665.

Munir, M.T., Kheirkhah, H., Baroutian, S., Quek, S.Y., Young, B.R., 2018. Subcritical water extraction of bioactive compounds from waste onion skin. J. Clean. Prod. 183, 487–494. https://doi.org/10.1016/j.jclepro.2018.02.166.

Nuissier, G., Bourgeois, P., Grignon-Dubois, M., Pardon, P., Heíè Ne Lescure, M., n.d. Composition of sugarcane waxes in rum factory wastes.

Oliveira, G., Gonçalves, I., Barra, A., Nunes, C., Ferreira, P., Coimbra, M.A., 2020. Coffee silverskin and starch-rich potato washing slurries as raw materials for elastic, antioxidant, and UV-protective biobased films. Food Res. Int. 138. https://doi.org/10.1016/j.foodres.2020.109733.

Oliveira, G., Passos, C.P., Ferreira, P., Coimbra, M.A., Gonçalves, I., 2021. Coffee by-products and their suitability for developing active food packaging materials. Foods. https://doi.org/10.3390/foods10030683.

Pagano, C., Marinozzi, M., Baiocchi, C., Beccari, T., Calarco, P., Ceccarini, M.R., Chielli, M., Orabona, C., Orecchini, E., Ortenzi, R., Ricci, M., Scuota, S., Tiralti, M.C., Perioli, L., 2020. Bioadhesive polymeric films based on red onion skins extract for wound treatment: an innovative and eco-friendly formulation. Molecules 25. https://doi.org/10.3390/molecules25020318.

Petronilho, S., Oliveira, A., Domingues, M.R., Nunes, F.M., Coimbra, M.A., Gonçalves, I., 2021. Hydrophobic starch-based films using potato washing slurries and spent frying oil. Foods 10. https://doi.org/10.3390/foods10122897.

Pucciarini, L., Ianni, F., Petesse, V., Pellati, F., Brighenti, V., Volpi, C., Gargaro, M., Natalini, B., Clementi, C., Sardella, R., 2019. Onion (Allium cepa L.) Skin: a rich resource of biomolecules for the sustainable production of colored biofunctional textiles. Molecules 24. https://doi.org/10.3390/molecules24030634.

Putnik, P., Gabrić, D., Roohinejad, S., Barba, F.J., Granato, D., Mallikarjunan, K., Lorenzo, J.M., Bursać Kovačević, D., 2019. An overview of organosulfur compounds from Allium spp.: from processing and preservation to evaluation of their bioavailability, antimicrobial, and anti-inflammatory properties. Food Chem. https://doi.org/10.1016/j.foodchem.2018.10.068.

Sagar, N.A., Khar, A., Vikas, T., Pareek, A., 2021. Physicochemical and thermal Characteristics of Onion Skin from fifteen Indian Cultivars for possible Food applications. J. Food Qual. 2021. https://doi.org/10.1155/2021/7178618.

Santos, L.G., Silva, G.F.A., Gomes, B.M., Martins, V.G., 2021. A novel sodium alginate active films functionalized with purple onion peel extract (Allium cepa). Biocatal. Agric. Biotechnol. 35. https://doi.org/10.1016/j.bcab.2021.102096.

Serra, I.R., Fradique, R., Vallejo, M.C.S., Correia, T.R., Miguel, S.P., Correia, I.J., 2015. Production and characterization of chitosan/gelatin/β-TCP scaffolds for improved bone tissue regeneration. Mater. Sci. Eng. C 55, 592–604. https://doi.org/10.1016/j.msec.2015.05.072.

Shabir, I., Pandey, V.K., Dar, A.H., Pandiselvam, R., Manzoor, S., Mir, S.A., Shams, R., Dash, K.K., Fayaz, U., Khan, S.A., Jeevarathinam, G., Zhang, Y., Rusu, A.V., Trif, M., 2022. Nutritional Profile, Phytochemical Compounds, Biological Activities, and Utilisation of Onion Peel for Food applications: a Review. Sustainability (switzerland). https://doi.org/10.3390/su141911958.

Shafiq, S., Al-Maythalony, B.A., Usman, M., Ba-Shammakh, M.S., Al-Shammari, A.A., 2021. ZIF-95 as a filler for enhanced gas separation performance of polysulfone membrane. RSC Adv. 11, 34319–34328. https://doi.org/10.1039/d1ra06271a.

Singh, G.P., Bangar, S.P., Yang, T., Trif, M., Kumar, V., Kumar, D., 2022. Effect on the Properties of Edible Starch-based Films by the Incorporation of Additives: a Review. Polymers (basel). https://doi.org/10.3390/polym14101987.

Singh, R., Kaur, S., Sachdev, P.A., 2021. A cost effective technology for isolation of potato starch and its utilization in formulation of ready to cook, non cereal, and non glutinous soup mix. J. Food Meas. Charact. 15, 3168–3181. https://doi.org/10.1007/s11694-021-00887-w.

Stoica, F., Constantin, O.E., Stănciuc, N., Aprodu, I., Bahrim, G.E., Răpeanu, G., 2022. Optimization of the Parameters Influencing the Antioxidant activity and Concentration of Anthocyanins Extracted from Red Onion Skins using a Central Composite Design. Inventions 7. https://doi.org/10.3390/inventions7040089.

Tester, R.F., Karkalas, J., Qi, X., 2004. Starch - Composition, fine structure and architecture. J. Cereal Sci. https://doi.org/10.1016/j.jcs.2003.12.001.

Thivya, P., Bhosale, Y.K., Anandakumar, S., Hema, V., Sinija, V.R., 2022. Study on the characteristics of gluten/alginate-cellulose/onion waste extracts composite film and its food packaging application. Food Chem. 390. https://doi.org/10.1016/j.foodchem.2022.133221.

Uçak, İ., Yerlikaya, P., Khalily, R., Abuibaid, A.K.M., 2019. Effects of Gelatin Edible Films Containing Onion Peel Extract on the Quality of Rainbow Trout Fillets. Eurasian Journal of Food Science and Technology.

Wang, C., Lu, Y., Li, Z., An, X., Gao, Z., Tian, S., 2022a. Preparation and Performance Characterization of a Composite Film based on Corn Starch, κ-Carrageenan, and Ethanol Extract of Onion Skin. Polymers (basel) 14. https://doi.org/10.3390/polym14152986.

Wang, C., Tian, S., Gao, Z., Li, Z., An, X., Lu, Y., Song, Y., Zhao, Y., 2022b. Preparation and characterization of chitosan-based antioxidant composite films containing onion skin ethanolic extracts. J. Food Meas. Charact. 16, 598–609. https://doi.org/10.1007/s11694-021-01187-z.

Waterschoot, J., Gomand, S.V., Fierens, E., Delcour, J.A., 2015. Production, structure, physicochemical and functional properties of maize, cassava, wheat, potato and rice starches. Starch/Staerke. https://doi.org/10.1002/star.201300238.

Wolf, C., Angellier-Coussy, H., Gontard, N., Doghieri, F., Guillard, V., 2018. How the shape of fillers affects the barrier properties of polymer/non-porous particles nanocomposites: a review. J Memb Sci. https://doi.org/10.1016/j.memsci.2018.03.085.

Zabihzadeh Khajavi, M., Ebrahimi, A., Yousefi, M., Ahmadi, S., Farhoodi, M., Mirza Alizadeh, A., Taslikh, M., 2020. Strategies for Producing Improved Oxygen Barrier Materials Appropriate for the Food Packaging Sector. food engineering reviews. Doi: 10.1007/s12393-020-09235-y/Published.